ARTICLE

Phase Transformations during Sintering of Titania Nanoparticles

Vishal N. Koparde[†,‡,*] and Peter T. Cummings[†]

[†]Department of Chemical Engineering, Vanderbilt University, Nashville, Tennessee 37235, and [‡]Department of Medicinal Chemistry, Virginia Commonwealth University, Richmond, Virginia 23219

ABSTRACT The size below which anatase nanoparticles become more stable than rutile nanoparticles (crossover diameter) is dependent on the environment of the nanoparticles. It is smaller for nanoparticles in vacuum than those in water and continues to decrease with increase in temperature. Phase transformation between anatase and rutile phases is facilitated by enhanced ionic mobility at temperatures near the melting point of the nanoparticles. Multiparticle multiphase molecular dynamics simulations of TiO_2 nanoparticles undergoing sintering-induced phase transformations are reported here. Over the time scales accessible to molecular dynamics simulations, we found that the final sintering agglomerate transformed to the rutile phase, provided one of the sintering nanoparticles was rutile, while sintering of anatase and amorphous nanoparticles resulted in a brookite agglomerate. No such phase transformations were observed at temperatures away from nanoparticle's melting temperatures.

KEYWORDS: anatase · rutile · titania nanoparticles · phase transformation · phase stability · molecular dynamics simulation

TiO_2 occurs naturally in rutile, anatase, and brookite crystal phases (or polymorphs). Rutile is the only stable phase in the bulk form, while bulk brookite and bulk anatase are metastable and transform irreversibly to rutile upon heating. However, relative phase stability at the nanoscale can be expected to be different than in the bulk. Phase transformations between different phases of TiO_2 have been extensively studied from both scientific and technological points of view.[1–13] Many attempts have been made to understand and control the anatase-to-rutile transformation as these phases have very different physical properties in the nanometer range. For example, nanoanatase is more photocatalytically active than nanorutile.[14–16] Numerous factors affect the anatase-to-rutile transformation. It has been reported[17] that the presence of certain dopants assists the anatase-to-rutile transition, while others help the anatase phase to be stable even at elevated temperatures. In solution, a decrease in pH is believed to favor the anatase-to-rutile transformation.[6,18] Similarly, surface effects can be expected to affect the anatase-to-rutile crossover diameter, that is, the particle size below which anatase is more stable than rutile. Apart from the particle size, the physical environment is one of the most significant factors controlling the relative phase stability of TiO_2 nanoparticles.

It is believed that the transformation from anatase-to-rutile upon heating is due to the increase in particle size due to the enhanced sintering at elevated temperatures. Experimental data[19,20] obtained at temperatures ranging between 598 and 1023 K suggest that anatase is the most stable phase at particle sizes under 11 nm, brookite is the most stable phase between 11 and 35 nm, while rutile is the most stable phase at all particle sizes above 35 nm. Thus, for larger nanoparticles, brookite would directly transform to rutile while anatase may transform directly either to rutile or to brookite and then to rutile. Naicker and coworkers[21] obtained qualitatively similar dependence of phase stability on particle size *via* molecular dynamics simulations of TiO_2 nanoparticles at 300 K in vacuum and reported a crossover of phase stability at ~2.5 nm. The authors attribute the disagreement between the simulation results and experiment may be due to limitations in the force fields used in the simulations, but we believe that the fact that these simulations were conducted in vacuum may have a significant impact on the anatase-to-rutile crossover diameter. *Ab initio* calculations[22–24] suggest that the crossover diameter is smaller for particles in vacuum than those in water, and that consideration of the appropriate surfacepassivation of the nanocrystalline surfaces is es-

*Address correspondence to vishal.koparde@alumni.vanderbilt.edu.

Received for review February 13, 2008 and accepted July 09, 2008.

Published online July 24, 2008.
10.1021/nn800092m CCC: $40.75

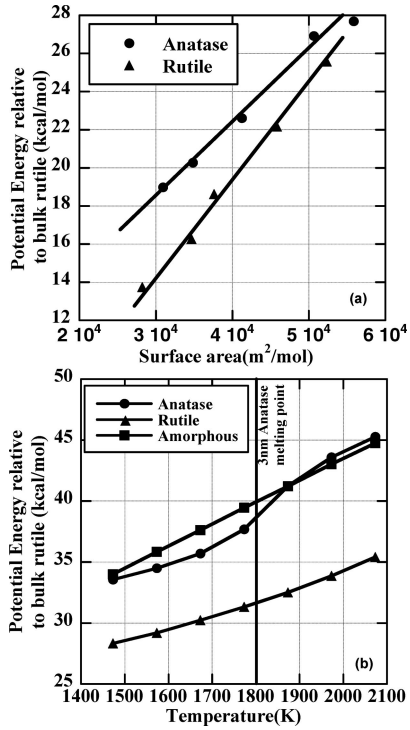

Figure 1. (a) Potential energy *versus* surface area of anatase and rutile nanoparticles at 1473 K. (b) Variation of potential energy with temperature for 3 nm anatase, rutile, and amorphous nanoparticles.

sential to accurately predict the size dependence of the anatase-to-rutile transformation.

RESULTS AND DISCUSSION

The energies of spherical TiO_2 nanoparticles ranging from 2.5 to 5nm in diameter measured *via* molecular dynamics (MD) simulations in vacuum at 1473 K are reported in Figure 1a. This temperature is comparable to the temperature prevailing in the flame reactors manufacturing TiO_2 nanoparticles *via* direct oxidation of $TiCl_4$.[25–27] On linear extrapolation, a crossover can be estimated at 1.65 (±0.25) nm; that is, particles smaller than ~1.65 nm are more stable as anatase, while those larger than ~1.65 nm are stable as rutile. Naicker *et al.* report a value ~2.5 nm at 300 K.[21] Thus, it is evident that as the temperature is increased the crossover diameter for anatase-to-rutile phase transformation in vacuum decreases, thereby suggesting that in vacuum at higher temperatures rutile nanoparticles are more stable than anatase nanoparticles down to lower nanoparticle diameters. To further justify this, we plot the trends in the potential energies of 3 nm anatase, rutile, and amorphous TiO_2 nanoparticles in vacuum as the temperature is increased in Figure 1b. It is observed that the relative stability of the rutile phase gradually increases with increasing temperature. Recently, we have also reported the melting points of these nanoparticles calculated using MD simulations,[28] which suggest that the simulation temperatures used here are very close to the melting points of 3 nm TiO_2 nanoparticles.

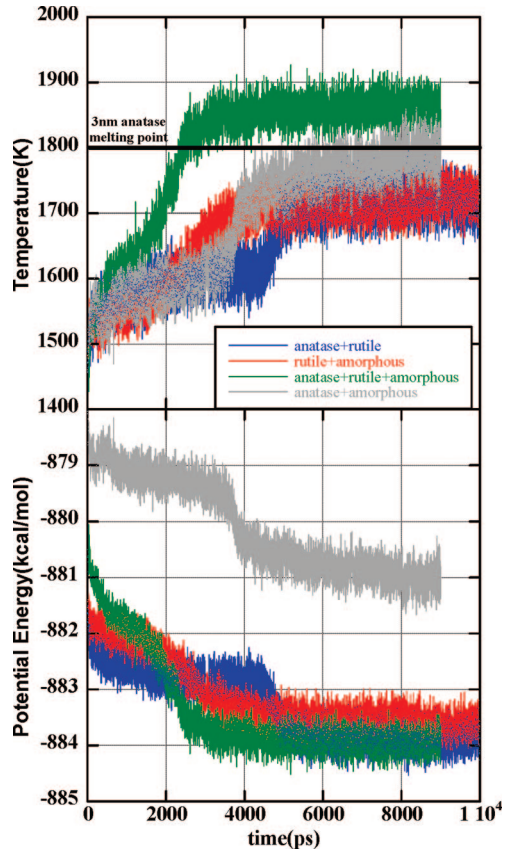

Figure 2. Temperature and configurational energy variations for various 3 nm sintering simulations.

It is important to note that at 1473 K both anatase and rutile are below their respective melting temperatures.

The multiparticle sintering simulations show that the nanoparticles are mutually attracted toward each other and form a neck, which gradually grows with time. The surface area of the coalescing nanoparticles, and thus the surface energy, decreases upon neck formation and growth. As the simulations are carried out in a microcanonical ensemble, the total energy of the system is conserved. Thus, a decrease in surface potential energy is accompanied by a corresponding equivalent change in the kinetic energy, which is evidenced by an increase in the system temperature. The temperature profiles for various simulations starting at 1473 K are shown in Figure 2 along with corresponding decrease in configurational energy of the system. A temperature increase ranging from 200 to 400 K is observed, with the highest increase for the simulation involving three nanoparticles.

Snapshots from the anatase + rutile simulations are shown in Figure 3, and the movie S1 is included in the Supporting Information. It is observed that as the sintering proceeds, a rutile front is moving into the anatase particle and an anatase-to-rutile transition takes place. Simulated X-ray diffraction patterns from Figure 4a indicate that the rutile phase becomes predominant as the sintering progresses. It is believed that if the simulation is continued for a very long period of time

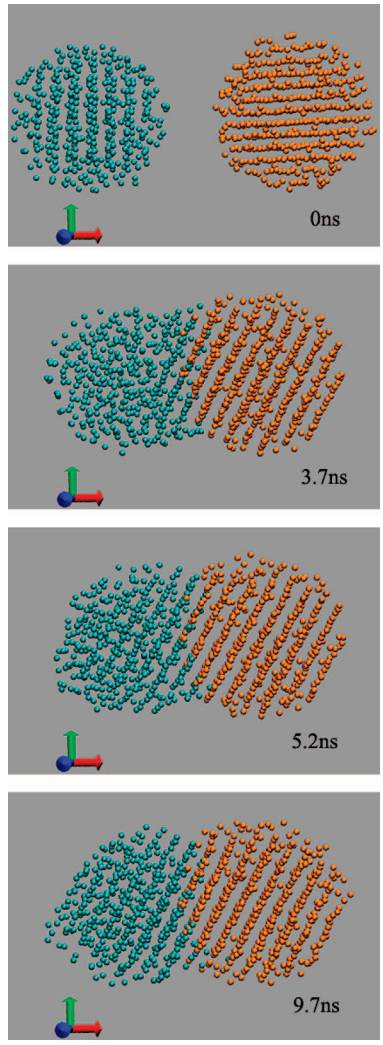

Figure 3. Snapshots from 3 nm anatase + 3 nm rutile simulation with a starting temperature of 1473 K. Only the titatium ions (blue for anatase, orange for rutile) are shown for clarity. The diameters of the titanium ions are drawn at a reduced scale in order to allow the reader to see underlying layers.

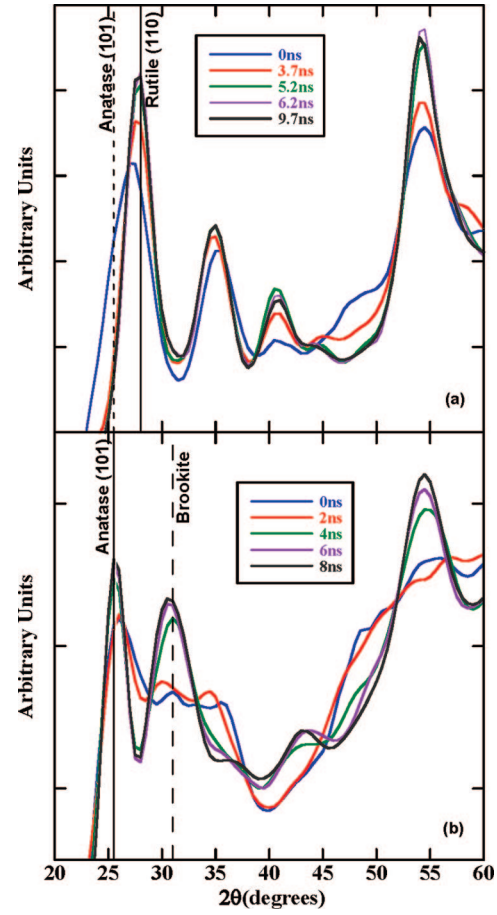

Figure 4. Simulated X-ray diffraction patterns of (a) anatase + rutile and (b) anatase + amorphous simulations.

then a single structurally relaxed (*i.e.*, approximately spherical) rutile particle will be obtained. Similar transformations to rutile phase are observed in simulations involving amorphous + rutile nanoparticles and those with anatase + amorphous + rutile nanoparticles. The snapshots of these simulations are not shown here for brevity but entire movies (S2 and S3) showing these sintering simulations are included in the Supporting Information). Thus, whenever one of the sintering nanoparticles is in the rutile phase, we conclude that the final agglomerate will be in the rutile phase. In case of the anatase + amorphous simulation, no rutile phase is initially present in the system. Careful examination of the simulated X-ray diffraction patterns, which are reported in Figure 4b, reveals that phase transformation does occur upon sintering, but the resultant phase at the end of 10 ns is brookite, the third polymorph of titania. [Please refer to movie S4 in the Supporting Information.] We believe that if this simulation is continued for a very long period of time then another phase transformation to the energetically more stable rutile phase will be observed, but this is beyond the scope of the molecular dynamics simulation reported here.

For comparison, all the simulations were repeated at 973 K. In each case, the particles underwent neck formation and the system temperature increased to about 1100 K, but no phase transformation was observed over the time scales considered. The fact that the maximum system temperatures reached over the periods of these simulations remained ~700 K below the calculated melting point of 3 nm anatase[28] is believed to be responsible for the absence of any observable phase transformation over the time scale of the MD simulation.

To summarize, the phase stability of TiO_2 nanoparticles is greatly dependent on their physical environment along with their size. For instance, the phase stability in water is different than the phase stability in vacuum for TiO_2 nanoparticles of the same size.[23,29] Zhang and Banfield[20] have reported that TiO_2 nanoparticles with diameter smaller than 11 nm are stable as anatase in water. However, our MD simulations show that this diameter is smaller if the nanoparticles are in vacuum and becomes smaller if the temperature is elevated, thereby suggesting that rutile is the most stable phase for

smaller TiO_2 nanoparticles at higher temperatures in vacuum.

The multiparticle multiphase simulations with system temperatures close to the melting points of the nanoparticles showed phase transformations over the course of nanoparticle sintering. Thus, the enhanced ionic mobility in nanoparticles close to their melting points plays a vital role in assisting phase transformations. For all such simulations, if any of the nanoparticles in the system were rutile, then the final agglomerate gradually transformed to rutile phase over ~10 ns. For anatase + amorphous simulation with a starting temperature of 1473 K, a brookite agglomerate was obtained at the end of 10 ns, which we believe will transform to rutile if the simulation is continued for a much longer period of time. This seems to suggest that anatase transforms to rutile directly if a rutile seed is present in the system and transforms to rutile *via* brookite in the absence of a rutile seed. For simulations starting at 973 K, system temperatures always remained much lower than the melting temperatures of the TiO_2 nanoparticles during the course of sintering and no phase transformations were observed. Incomplete anatase-to-rutile transformations during sintering of larger nanoparticles have been experimentally observed earlier.[30] However, we believe that the simulations reported here are the first observed phase transformations during nanoparticle sintering using MD simulations.

METHODS

The general purpose MD simulation package, DL_POLY[31,32] version 2.14, was used to perform all the simulations reported here. The Ti and O ions in the simulations are modeled as partially charged rigid spheres using the Matsui-Akaogi force field.[33] An analysis similar to that reported by Naicker *et al.*,[21] involving simulations of single anatase and rutile nanoparticles ranging from 2.5 to 5 nm in vacuum, was conducted at a higher temperature of 1473 K. The surface areas of the nanoparticles reported in Figure 1a are calculated using the Meyer method.[34] In addition to these simulations, we performed numerous multiparticle (2 or 3 particles) constant volume/constant energy (NVE) MD simulations at 1473 K involving 3 nm nanoparticles. The various combinations of phases involved in any particular simulation were (a) anatase + rutile, (b) amorphous + rutile, (c) anatase + amorphous + rutile, and (d) anatase + amorphous. These simulations were repeated at 973 K, which is well below the melting point of 3 nm anatase nanoparticles.[28] The particles were separated by a surface-to-surface gap of 1 nm at the beginning of each simulation. No periodic boundary conditions were employed, thus simulating isolated particles. All the Ti and O ions in the nanoparticles were included in the calculation of long-range electrostatic interactions (*i.e.*, no cutoff was employed), and no external forces were exerted on the particles to induce sintering. All simulations were run for at least 10 ns with a time step of 0.5 fs. Simulated X-ray diffraction patterns were used to detect any possible phase transformations. The calculation of the simulated X-ray diffraction pattern is reported elsewhere.[35]

Supporting Information Available: Movies S1−S4 of sintering TiO_2 nanoparticle simulation are available. It should be noted that the oxygen ions in the nanoparticles are not shown in all the movies for clarity. In these movies, Ti ions in rutile nanoparticles are orange, those in anatase are colored blue, while Ti in amorphous nanoparticles are shown in green. The coloring of the ions is based on the crystal structure of the nanoparticle that they belong to at the beginning of the simulation. The diameters of the ions are drawn at a reduced scale in order to allow the viewer to see the underlying layers and ordering. This material is available free of charge *via* the Internet at http://pubs.acs.org.

REFERENCES AND NOTES

1. Ahn, J. P.; Park, J. K.; Kim, G. Effect of Compact Density on Phase Transition Kinetics from Anatase Phase to Rutile Phase During Sintering of Ultrafine Titania Powder Compacts. *Nanostruct. Mater.* **1998**, *10*, 1087–1096.
2. Bakardjieva, S.; Stengl, V.; Szatmary, L.; Subrt, J.; Lukac, J.; Murafa, N.; Niznansky, D.; Cizek, K.; Jirkovsky, J.; Petrova, N. Transformation of Brookite-Type TiO_2 Nanocrystals to Rutile: Correlation between Microstructure and Photoactivity. *J. Mater. Chem.* **2006**, *16*, 1709–1716.
3. Borkar, S. A.; Dharwadkar, S. R. Temperatures and Kinetics of Anatase to Rutile Transformation in Doped TiO_2 Heated in Microwave Field. *J. Therm. Anal.* **2004**, *78*, 761–767.
4. Cerrato, G.; Marchese, L.; Morterra, C. Structural and Morphological Modifications of Sintering Microcrystalline TiO_2: An XRD, HRTEM and FTIR Study. *Appl. Surf. Sci.* **1993**, *70−71*, 200–205.
5. Gouma, P. I.; Mills, M. J. Anatase-to-Rutile Transformation in Titania Powders. *J. Am. Ceram. Soc.* **2001**, *84*, 619–622.
6. Hu, Y.; Tsai, H. L.; Huang, C. L. Phase Transformations of Precipitated TiO_2 Nanoparticles. *Mater. Sci. Eng., A* **2003**, *344*, 209–214.
7. Kim, J. Y.; Kim, D. W.; Jung, H. S.; Hong, K. S. Influence of Anatase-Rutile Phase Transformation on Dielectric Properties of Sol−Gel Derived TiO_2 Thin Films. *Jpn. J. Appl. Phys. Part 1* **2005**, *44*, 6148–6151.
8. Kumar, K. N. P. Growth of Rutile Crystallites During the Initial-Stage of Anatase-to-Rutile Transformation in Pure Titania and in Titania-Alumina Nanocomposites. *Scr. Metall. Mater.* **1995**, *32*, 873–877.
9. Kumar, K. N. P.; Keizer, K.; Burggraaf, A. J.; Okubo, T.; Nagamoto, H.; Morooka, S. Densification of Nanostructured Titania Assisted by a Phase-Transformation. *Nature* **1992**, *358*, 48–51.
10. Lu, H. M.; Zhang, W. X.; Jiang, Q. Phase Stability of Nanoanatase. *Adv. Eng. Mater.* **2003**, *5*, 787–788.
11. Machado, N.; Santana, V. S. Influence of Thermal Treatment on the Structure and Photocatalytic Activity of TiO_2-P25. *Catal. Today* **2005**, *107−108*, 595–601.
12. Nair, J.; Nair, P.; Mizukami, F.; Oosawa, Y.; Okubo, T. Microstructure and Phase Transformation Behavior of Doped Nanostructured Titania. *Mater. Res. Bull.* **1999**, *34*, 1275–1290.
13. Suresh, C.; Biju, V.; Mukundan, P.; Warrier, K. G. K. Anatase to Rutile Transformation in Sol−Gel Titania by Modification of Precursor. *Polyhedron* **1998**, *17*, 3131–3135.
14. Panpranot, J.; Kontapakdee, K.; Praserthdam, P. Effect of TiO_2 Crystalline Phase Composition on the Physicochemical and Catalytic Properties of Pd/ TiO_2 in Selective Acetylene Hydrogenation. *J. Phys. Chem. B* **2006**, *110*, 8019–8024.
15. Wahi, R. K.; Yu, W. W.; Liu, Y. P.; Mejia, M. L.; Falkner, J. C.; Nolte, W.; Colvin, V. L. Photodegradation of Congo Red Catalyzed by Nanosized TiO_2. *J. Mol. Catal. A: Chem.* **2005**, *242*, 48–56.
16. Choi, H.; Stathatos, E.; Dionysiou, D. D. Effect of Surfactant in a Modified Sol on the Physiochemical Properties and

Photocatalytic Activity of Crystalline TiO_2 Nanoparticles. *Top. Catal.* **2007**, *44*, 415–521.
17. Reidy, D. J.; Holmes, J. D.; Morris, M. A. The Critical Size Mechanism for the Anatase to Rutile Transformation in TiO_2 and Doped-TiO_2. *J. Eur. Ceram. Soc.* **2006**, *26*, 1527–1534.
18. Hu, Y.; Tsai, H. L.; Huang, C. L. Effect of Brookite Phase on the Anatase-Rutile Transition in Titania Nanoparticles. *J. Eur. Ceram. Soc.* **2003**, *23*, 691–696.
19. Ranade, M. R.; Navrotsky, A.; Zhang, H. Z.; Banfield, J. F.; Elder, S. H.; Zaban, A.; Borse, P. H.; Kulkarni, S. K.; Doran, G. S.; Whitfield, H. J. Energetics of Nanocrystalline TiO_2. *Proc. Natl. Acad. Sci. U.S.A.* **2002**, *99*, 6476–6481.
20. Zhang, H. Z.; Banfield, J. F. Understanding Polymorphic Phase Transformation Behavior during Growth of Nanocrystalline Aggregates: Insights from TiO_2. *J. Phys. Chem. B* **2000**, *104*, 3481–3487.
21. Naicker, P. K.; Cummings, P. T.; Zhang, H. Z.; Banfield, J. F. Characterization of Titanium Dioxide Nanoparticles Using Molecular Dynamics Simulations. *J. Phys. Chem. B* **2005**, *109*, 15243–15249.
22. Barnard, A. S.; Zapol, P. Predicting the Energetics, Phase Stability, and Morphology Evolution of Faceted and Spherical Anatase Nanocrystals. *J. Phys. Chem. B* **2004**, *108*, 18435–18440.
23. Barnard, A. S.; Zapol, P.; Curtiss, L. A. Modeling the Morphology and Phase Stability of TiO_2 Nanocrystals in Water. *J. Chem. Theory Comput.* **2005**, *1*, 107–116.
24. Barnard, A. S.; Zapol, P. Effects of Particle Morphology and Surface Hydrogenation on the Phase Stability of TiO_2. *J. Phys.: Condens. Matter* **2004**, *70*, 235403.
25. Akhtar, M. K.; Yun, X. O.; Pratsinis, S. E. Vapor Synthesis of Titania Powder by Titanium Tetrachloride Oxidation. *AIChE J.* **1991**, *37*, 1561–1570.
26. Jang, H. D.; Jeong, J. The Effects of Temperature on Particle-Size in the Gas-Phase Production of TiO_2. *Aerosol Sci. Technol.* **1995**, *23*, 553–560.
27. Kobata, A.; Kusakabe, K.; Morooka, S. Growth and Transformation of TiO_2 Crystallites in Aerosol Reactor. *AIChE J.* **1991**, *37*, 347–359.
28. Koparde, V. N.; Cummings, P. T. Sintering of Titanium Dioxide Nanoparticles: A Comparison between Molecular Dynamics and Phenomenological Modeling. *J. Nanopart. Res.* **2008**, in press DOI: 10.1007/s11051-007-9342-3.
29. Koparde, V. N.; Cummings, P. T. Molecular Dynamics Study of Water Adsorption on TiO_2 Nanoparticles. *J. Phys. Chem. C* **2007**, *111*, 6920–6926.
30. Bykov, Y.; Gusev, S.; Eremeev, A.; Holoptsev, V.; Malygin, N.; Pivarunas, S.; Sorokin, A.; Shurov, A. Sintering of Nanophase Oxide Ceramics by Using Millimeter-Wave Radiation. *Nanostruct. Mater.* **1995**, *6*, 855–858.
31. Smith, W. CCP5: A Collaborative Computational Project for the Computer Simulation of Condensed Phases. *J. Mol. Graphics* **1987**, *5*, 71–74.
32. Smith, W.; Forester, T. R. Dl_Poly_2.0: A General-Purpose Parallel Molecular Dynamics Simulation Package. *J. Mol. Graphics* **1996**, *14*, 136–141.
33. Matsui, M.; Akaogi, M. Molecular Dynamics Simulation of the Structural and Physical Properties of the Four Polymorphs of TiO_2. *Mol. Sim.* **1991**, *6*, 239–244.
34. Meyer, A. Y. Molecular Mechanics and Molecular Shape. V. On the Computation of the Bare Surface Area of Molecules. *J. Comput. Chem.* **1988**, *9*, 18–24.
35. Koparde, V. N.; Cummings, P. T. Molecular Dynamics Simulation of Titanium Dioxide Nanoparticle Sintering. *J. Phys. Chem. B* **2005**, *109*, 24280–24287.